Bioorganic & Medicinal Chemistry Letters 19 (2009) 2924–2927

Contents lists available at ScienceDirect

Bioorganic & Medicinal Chemistry Letters

journal homepage: www.elsevier.com/locate/bmcl

Optimization of pyrazole inhibitors of Coactivator Associated Arginine Methyltransferase 1 (CARM1)

Tram Huynh [a], Zhong Chen [a], Suhong Pang [a], Jieping Geng [a], Tiziano Bandiera [b,†], Simona Bindi [b], Paola Vianello [b], Fulvia Roletto [b], Sandrine Thieffine [b], Arturo Galvani [b], Wayne Vaccaro [a], Michael A. Poss [a], George L. Trainor [a], Matthew V. Lorenzi [a], Marco Gottardis [a], Lata Jayaraman [a], Ashok V. Purandare [a,*]

[a] Bristol-Myers Squibb Pharmaceutical Research and Development, Princeton, NJ 08543, United States
[b] Nerviano Medical Sciences Oncology Business Unit, Viale Pasteur, 20014 Nerviano, Milan, Italy

ARTICLE INFO

Article history:
Received 21 March 2009
Revised 9 April 2009
Accepted 17 April 2009
Available online 22 April 2009

Keywords:
Coactivator associated arginine methyltransferase 1
CARM1
PRMT4
Pyrazole
Methyltransferase

ABSTRACT

Design, synthesis, and SAR development led to the identification of the potent, novel, and selective pyrazole based inhibitor (**7f**) of Coactivator Associated Arginine Methyltransferase (CARM1).

© 2009 Elsevier Ltd. All rights reserved.

Protein arginine methyl transferase (PRMT) family members have been shown to play a role in various cellular processes including nuclear hormone receptor (NHR) mediated signaling, protein–protein interactions, protein trafficking, mRNA splicing and processing and transcriptional regulation.[1] The family, consisting of at least 9 members (PRMTs 1–9), catalyze the generation of dimethyl arginine residues on substrate proteins.[2] CARM1 (or PRMT4), has been shown to methylate arginine residues asymmetrically in a wide variety of substrate proteins such as histone H3, p300/CBP, U1C, SAP49, CA150, HuR, HuD and PABP. These events affect chromatin architecture which impacts transcriptional initiation, alternative splicing, mRNA processing and stabilization.[3–5] Taken together, these observations point to a crucial role for CARM1 in modulating gene expression at multiple critical levels. Lately, CARM1 has been shown to be up-regulated during the progression of prostate cancer.[6] Over-expression of CARM1 is seen in both androgen-stimulated and castration resistant prostate cancer tumors. A convincing argument can therefore be made to support the hypothesis that targeting CARM1 would be a viable approach for anti-cancer therapy. Hence, the identification of selective CARM1 inhibitors as tools to interrogate its function in cells may be of significant interest.

To date, there have been only a few publications describing small molecule chemical modulators of the PRMTs.[7] Recently, we reported[8] Hits to Lead optimization studies leading to the identification of pyrazole analogs (**1** Fig. 1) as potent and selective inhibitors of CARM1.[9]

These studies had demonstrated that *meta-substituted (S)*-alanine benzyl amide is preferred at the South end whereas the SAR of the East end is more tolerant of substitution. Pyrazole **1** however showed only modest permeability (PAMPA Pc < 15 nm/s).[10] Herein,

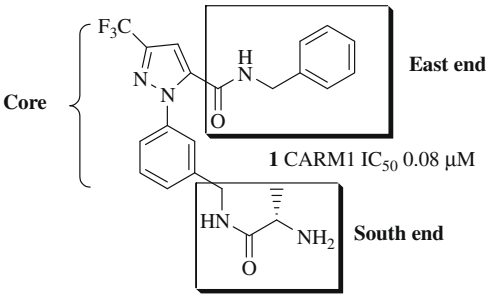

Figure 1.

* Corresponding author. Tel.: +1 609 252 4320; fax: +1 609 252 7446.
E-mail address: ashok.purandare@bms.com (A.V. Purandare).
† Current address: Italian Institute of Technology, Via Morego, 30 16163 Genova, Italy.

0960-894X/$ - see front matter © 2009 Elsevier Ltd. All rights reserved.
doi:10.1016/j.bmcl.2009.04.075

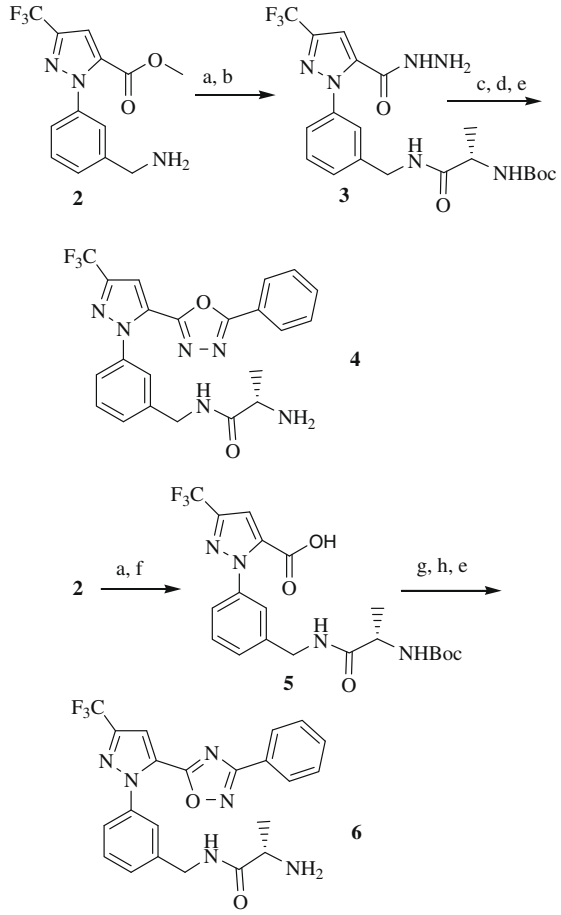

Scheme 1. Reagent and conditions: (a) Boc-L-Ala-OSu, CH_2Cl_2, Et_3N, 92%; (b) hydrazine hydrate, heat, 30 min, 80%; (c) benzoic acid, PyBOP, DIEA, DMF, rt; (d) DIC, DMF, microwave, 150 °C, 20 min, 60% from **3**; (e) TFA-CH_2Cl_2, 92%; (f) 1 N aq NaOH–MeOH, rt, 65%; (g) benamidoxime, CDI, DMF, rt, 4 h; (h) CDI, 100 °C, 4 h, 45% for combined g and h steps.

we report further optimization of the core and East end that led to the identification of a selective and potent pyrazole inhibitor (**7f**).

At the outset, we explored amide surrogates at the East end of the molecule to reduce hydrogen bond donors in order to improve the permeability. Towards this end, we first examined 1,3,4- and 1,2,4-oxadiazoles as amide surrogates. These surrogates were synthesized as shown in Scheme 1.

From this exercise, the 1,3,4-oxadiazole (**4**) was found to be preferred over the 1,2,4-regioisomer (**6**). This modification not only improved the in vitro potency versus amide (**1**), but also improved the permeability as measured in the PAMPA assay (Pc < 15 nm/s for **1** to 106 nm/s for **4**) (Table 1).

Encouraged by these findings, we examined additional substitutions at the 5-position of the 1,3,4-oxadiazole. These analogs were readily assembled using the protocol as shown in Scheme 2.

Among the various C-5 substitutions (only partial data shown, Table 2), aryl groups with *ortho*-substitution were found to be superior to either *meta*- or *para*-substitutions. Inclusion of a nitrogen atom in the ring (as in **7b**) was not tolerated. Interestingly, an

Table 1
SAR for amide surrogates

Compound[11]	CARM1 IC_{50}[9] (μM)
1	0.08
4	0.06
6	0.21

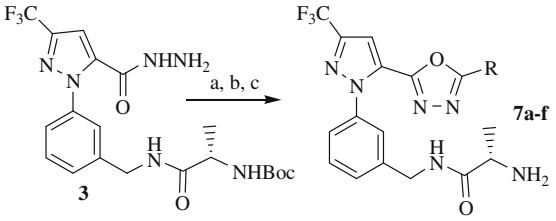

Scheme 2. Reagent and conditions: (a) RCO_2H, PyBOP, DIEA, DMF, rt or RNCO in case of **7g**; (b) DIC, DMF, microwave, 150 °C, 20 min; (c) TFA-CH_2Cl_2, 30–50% from **3**.

additional NH-linker (as in **7g**) was tolerated, however, this modification diminished the permeability (PAMPA Pc < 15 nm/s).

Next, we evaluated five-membered heterocyclic cores while retaining the relative disposition of the East and South ends with the same substitutions as in **4**. These analogs were prepared from the corresponding known intermediates (**8a–e**)[12] using the general approach as disclosed in Scheme 3.

A 3-trifluoromethyl substituted pyrazole was found to be the preferred core from the various five-membered heterocycles (Table 3). Among the remaining cores, heterocycles with an unhindered

Table 2
SAR for East end

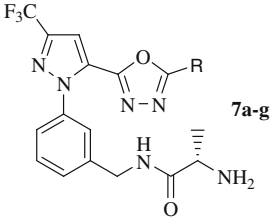

Compound[11]	R	CARM1 IC_{50}[9] (μM)
4	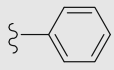	0.06
7a	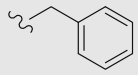	0.31
7b	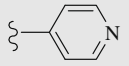	1.54
7c	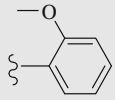	0.05
7d	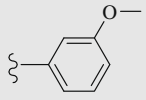	0.16
7e	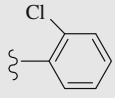	0.05
7f	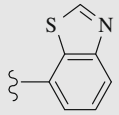	0.04
7g	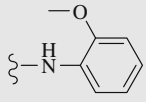	0.05

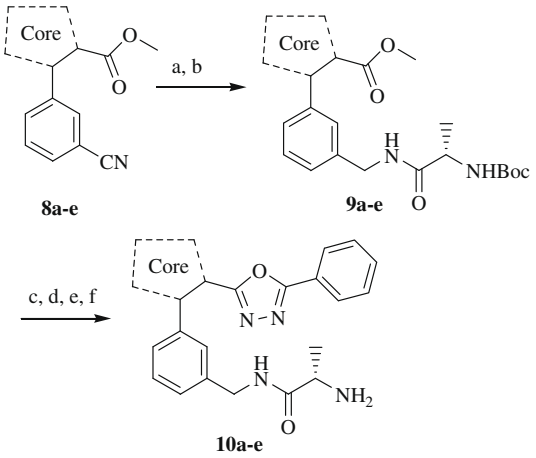

Scheme 3. Reagent and conditions: (a) H_2, 10%Pd/C, MeOH, 70–80%; (b) Boc-L-Ala-OSu, CH_2Cl_2, Et_3N, 85–95%; (c) hydrazine hydrate, heat, 30 min, 70–80%; (d) benzoic acid, PyBOP, DIEA, DMF, rt; (e) DIC, DMF, microwave, 150 °C, 20 min, 40–60% combined for d and e; (f) TFA-CH_2Cl_2, 80–93%.

hydrogen bond acceptor at the 2′ position were preferred (e.g., **10c** vs **10d**).

We also studied the effect of substitution of the amide nitrogen, and removal of the amide bond itself at the South end on CARM1 inhibition. Synthesis of these analogs was achieved as outlined in Scheme 4.

Table 3
SAR for core

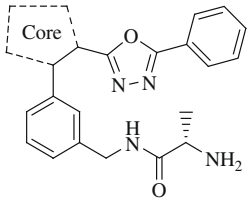

Compound[11]	Core	CARM1 IC_{50}[9] (μM)
4	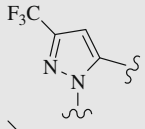	0.06
10a	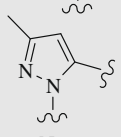	0.13
10b	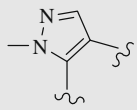	2.20
10c	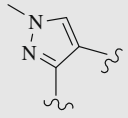	0.4
10d	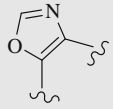	0.36
10e	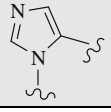	2.1

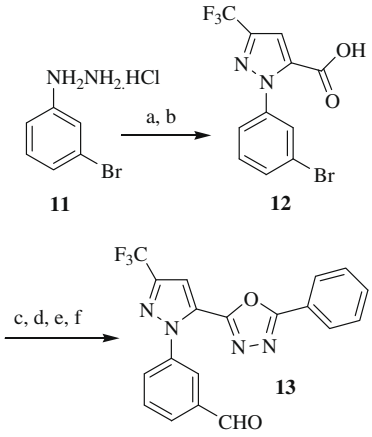

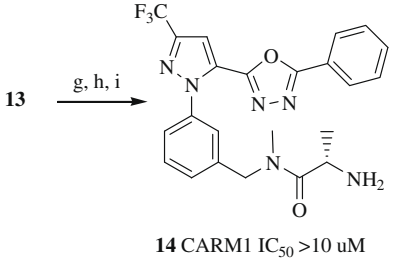

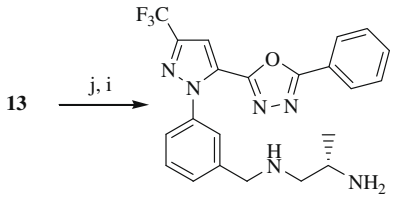

Scheme 4. Reagent and conditions: (a) 4,4,4-trifluoro-1-(furan-2-yl)butane-1,3-dione, AcOH, reflux, 84%; (b) $RuCl_3$, $NaIO_4$, CH_3CN–CH_2Cl_2–H_2O (2:2:3); (c) benzohydrazide, PyBOP, DIPEA, CH_2Cl_2, 59% for combined b and c; (d) DIC, DMF, 150 °C, 60%; (e) tributyl-(vinyl)stannane, $Pd(0)(PPh_3)_4$, toluene, 110 °C, 65%; (f) HCOOH, H_2O_2, HIO_4, 73%; (g) methylamine HCl, $Ti(OiPr)_4$, $NaBH_4$, EtOH, 50%; (h) Boc-Ala-OH, EDC·HCl, HOBt, DIPEA, DMF, 91%; (i) HCl-dioxane, 49–60%; (j) Boc-alaninal, NaH $B(OAc)_3$, THF, 60%.

Table 4
In vitro profiling of **7f**

Human microsome stability (nM/min/mg prot.)	**0.026**
PAMPA: Pc (nm/s)	267
hPXR[14] (EC_{50}, μM)	>25
HHA IC_{50}[15] (μM)	All >100

Both of these modifications (compounds **14** and **15**) led to a significant loss of potency compared to **4**, thereby reaffirming the earlier observation of little tolerance for changes at the South end of the molecule.

In order to assess the selectivity versus closely related PRMTs, we evaluated the most potent compound (**7f**) for its ability to inhibit PRMT1 and PRMT3.[13] Compound **7f** was found to be significantly less active against these enzymes (IC_{50} > 25 μM) suggesting selectivity in binding and inhibition. Compound **7f** showed acceptable profile in the in vitro panel (Table 4).

In summary, through SAR development and optimization of the core and East end of **1**, we have identified the pyrazole derivative **7f** as a potent and selective inhibitor of CARM1. Further work re-

lated to the utility of this class of inhibitors will be reported in due course.

References and notes

1. Krause, C.; Yang, Z.; Kim, Y.; Lee, J.; Cook, J.; Pestka, S. *Pharm. Ther.* **2007**, *113*, 50.
2. Zhang, Y.; Reinberg, D. *Genes Dev.* **2001**, *15*, 2343.
3. Chen, D.; Ma, H.; Hong, H.; Koh, S.; Huang, S.; Schurter, B.; Aswad, D.; Stallcup, M. *Science* **1999**, *284*, 2174; Xu, W.; Chen, H.; Du, K.; Asahara, H.; Tini, M.; Emerson, B.; Montimony, M.; Evans, R. *Science* **2001**, *294*, 2507; Chevillard-Briet, M.; Trouche, D.; Vandel, L. *EMBO J.* **2002**, *21*, 5457.
4. Cheng, D.; Cote, J.; Shaaban, S.; Bedford, M. *Mol. Cell* **2007**, *25*, 71.
5. Li, H.; Park, S.; Kilburn, B.; Jelinek, M.; Henschen-Edman, A.; Aswas, D.; Stallcup, M.; Laird-Offringa, I. *J. Biol. Chem.* **2002**, *277*, 44623; Lee, J.; Bedford, M. *EMBO Rep.* **2002**, *3*, 268; Fujiwara, T.; Mori, Y.; Chu, D.; Koyama, Y.; Miyata, Y.; Tanaka, H.; Yachi, K.; Kubo, T.; Yoshikawa, H.; Tohyama, M. *Mol. Cell Biol.* **2006**, *26*, 2273.
6. (a) Hong, H.; Kao, C.; Jeng, M.; Eble, J.; Koch, M.; Gardner, T.; Zhang, S.; Li, L.; Pan, C.; Hu, Z.; M, G.; Cheng, L. *Cancer* **2004**, *101*, 83; (b) Majumdar, S.; Liu, Y.; Ford, O.; Mohler, J.; Whang, Y. *Prostate.* **2006**, *66*, 1292.
7. (a) Cheng, D.; Yadav, N.; King, R. W.; Swanson, M. S.; Weinstein, E. J.; Bedford, M. T. *J. Biol. Chem.* **2004**, *279*, 23892; (b) Ragno, R.; Simeoni, S.; Castellano, S.; Vicidomini, C.; Mai, A.; Caroli, A.; Tramontano, A.; Bonaccini, C.; Trojer, P.; Bauer, I.; Brosch, G.; Sbardella, G. *J. Med. Chem.* **2007**, *50*, 1241; (c) Spannhoff, A.; Heinke, R.; Bauer, I.; Trojer, P.; Metzger, E.; Gust, R.; Schuele, R.; Brosch, G.; Sippl, W.; Jung, M. *J. Med. Chem.* **2007**, *50*, 2319; (d) Spannhoff, A.; Machmur, R.; Heinke, R.; Trojer, P.; Bauer, I.; Brosch, G.; Schule, R.; Hanefeld, W.; Sippl, W.; Jung, M. *Bioorg. Med. Chem. Lett.* **2007**, *17*, 4150; (e) Wahhab, A.; Therrien, E.; Allan, M.; Manku, S. WO2008104077.; (f) Allan, M.; Manku, S.; Therrien, E.; Nguyen, N.; Styhler, S.; Robert, M.; Goulet, A.; Petschner, A. J.; Rahil, G.; Robert, M. A.; Deziel, R.; Besterman, J. M.; Nguyen, H.; Wahhab, A. *Bioorg. Med. Chem. Lett.* **2009**, *19*, 1218.
8. Purandare, A. V.; Chen, Z.; Huynh, T.; Pang, S.; Geng, J.; Vaccaro, W.; Poss, M. A.; Oconnell, J.; Nowak, K.; Jayaraman, L. *Bioorg. Med. Chem. Lett.* **2008**, *18*, 4438.
9. A filter based assay as described in Ref. 8 utilizing histone H3 as substrate was used to test compounds that specifically detected CARM1 dependent methylation, and the values reported are average of three with <10% variability.
10. PAMPA assay—10 mM stocks of compound in 100% DMSO was used. Compounds are diluted 1:100 in pH 7.4 or pH 5.5 donor well buffer (pION CAT # 110151) providing a 100 μM assay solution in 1% DMSO. Compound diluted in donor well buffer is transferred to a Whatman Unifilter plate and filtered prior to dispensing 200 μl into the donor well of the assay plate (pION CAT #110163). The PAMPA membrane is formed by pipetting 4 μl of the lipid solution (pION CAT #110169) onto the filter plate (VWR CAT #13503). The membrane is then covered with 200 μl of acceptor well buffer at pH 7.4 (pION CAT #110139). The PAMPA assay plate (donor side and acceptor side) is combined and allowed to incubate at room temperature for 4 h. The plate is then disassembled and spectrophotometer plates (VWR CAT #655801) are filled (150 μl/well). The donor, acceptor, reference, and blank plates are read in the SpectraMax UV plate reader. Data is captured by the pION software which analyzes the spectra and generates Pc values.
11. (a) All compounds were characterized by LC–MS and NMR analysis. In addition, the yields were based on the weight of pure product unless mentioned otherwise. (b) Analytical data for compound **7b**: ^{1}H NMR (500 MHz, MeOH-*d*) δ ppm 9.41 (s, 1H), 8.34 (dd, *J* = 8.14, 0.88 Hz, 1H), 8.01 (d, *J* = 7.26 Hz, 1H), 7.77 (dd, *J* = 8.14, 7.70 Hz, 1H), 7.72 (s, 1H), 7.65 (br s, 1H), 7.57–7.62 (m, 3H), 4.59 (A of AB, *J* = 15.41 Hz, 1H), 4.55 (B of AB, *J* = 15.19 Hz, 1H), 3.96–4.03 (m, 1H), 1.53 (d, *J* = 7.04 Hz, 3H); MS (ESI) *m/z* 514.12 (M+H).
12. Fevig, J. M.; Pinto, D. J.; Han, Q.; Quan, M. L.; Pruitt, J. R.; Jacobson, I. C.; Galemmo, R. A., Jr.; Wang, S.; Orwat, M. J.; Bostrom, L. L.; Knabb, R. M.; Wong, P. C.; Lam, P. Y. S.; Wexler, R. R. *Bioorg. Med. Chem. Lett.* **2001**, *11*, 641.
13. PRMT1 and PRMT3 specific methylation assays were performed using assay conditions as reported in Ref. 8.
14. hPXR; Human pregnane-X receptor.
15. HHA: The Human Hepatocyte Assay. Compound **7f** showed IC_{50} > 100 μM for the parent cell line (Tc5) and all CYP transfected lines (3A4, 2C9, 2C19 and 2D6).